DOI: 10.61782/fa.2025.0048

FORUM ACUSTICUM
EURONOISE 2025

VIBRO-ACOUSTIC CALIBRATION FOR THE FEM SIMULATION OF A THIN-WALLED DUCT SYSTEM AND FAN HOUSING

Patrick Heidegger[1*] **Felix Czwielong**[2] **Stefan Schoder**[1]
Stefan Becker[2] **Manfred Kaltenbacher**[1]

[1] Institute of Fundamentals and Theory in Electrical Engineering, Graz University of Technology, Austria
[2] Institute of Fluid Mechanics, Friedrich-Alexander-University Erlangen-Nuremberg, Germany

ABSTRACT

Evaluating the acoustic behavior of a ducted ventilation system poses multiple challenges, e.g., possibly changing cross-sections, a lack of symmetry due to a non-straight layout, or a thin-walled structure acting as a bypass for sound waves traveling to the exterior. These aspects can be tackled via numerical simulation methods, like the finite element method, but uncertainties remain. Examples are the necessity to omit geometrical details for obtaining a computable model, the unknown and often non-ideal behavior of parts like the suspension or connecting joints, and unknown material properties. This proceeding discusses the calibration process for the vibroacoustic simulation of a thin-walled aluminum duct and a centrifugal-fan housing belonging to a high-precision aeroacoustic test rig.

Keywords: *centrifugal fan, finite element method, duct acoustics, model calibration*

1. INTRODUCTION

Centrifugal fans transport air and gases for industrial and civilian applications, e.g., in building ventilation systems. In ducted ventilation systems, the noise produced by the operating fan may propagate over wide distances within the ducts. The noise approaches the exterior field either via duct openings or by transmission through the duct walls (acoustic breakout) [1] and may constitute a source disturbance for potential listeners.

Acoustic breakout may contribute significantly to the total sound emission of the ducted ventilation system, depending on various parameters such as the construction material, the wall thickness, and the duct cross-section [2]. Understanding the vibroacoustic behavior of the duct can thus be essential for classifying the sound emission of a ducted ventilation system.

Numerical simulation methods are widely employed to gain such insights, but obtaining a valid computational model that reflects the actual real-world system poses multiple challenges. Examples are non-symmetric duct layouts, the necessity to omit geometrical details in the meshing process, the unknown and usually non-ideal behavior of mountings or connecting joints, and unknown material properties. For investigating the complex fluid-structure-acoustic interactions occurring in ducted centrifugal fans, a benchmark case for an academic centrifugal fan is being established in a research project. The benchmark case is an extension to the test rig proposed in [3] and covers simulations of the fluid mechanical, structural mechanical, and acoustic fields, accompanied by extensive measurements of all three physical domains.

This work in progress describes the vibroacoustic finite-element (FE) model of the fan housing, the duct walls, and the surrounding air of the benchmark case. Further, two approaches for tuning the simulation models to reference measurements are discussed. One refers to laser-vibrometry scans on parts of the mechanical structure excited by an impact hammer (method 1). The other refers to exterior microphone signals, excited via a voice-coil loudspeaker attached to the duct end (method 2).

**Corresponding author*: patrick.heidegger@tugraz.at.

2. EXPERIMENTAL SETUP

The housing of the test fan consists of an 8 mm aluminum sheet connected by flanges. The duct system is mainly made of a 2 mm aluminum sheet, connected by flanges or welded joints. It consists of a narrowing transition piece (close duct) mounted on the downstream side of the fan housing and an extension part with a constant cross-section (extended duct). The two duct parts are connected by a flexible connector (canvas sleeve) made of truck tarpaulin, which has the purpose of mitigating the coupling of mechanical vibrations between the parts. The test rig is located in an acoustically treated chamber to reduce the room-acoustic impact on the sound radiation of the structure. A photograph of the setup is depicted in Fig. 1.

A system identification was performed using two types of measurements. Method 1: an impact hammer was used to excite the structure on the front flange of the fan housing in the surface-normal direction. The vibration response was scanned on the front, upper, and lower surfaces of the fan housing and the closed duct by 3D laser-vibrometry. The back-side surfaces could not be scanned due to the limited space. Method 2: An enclosed voice-coil loudspeaker was installed on the end of the extended duct to excite the system, and the sound radiation was recorded in twelve different positions.

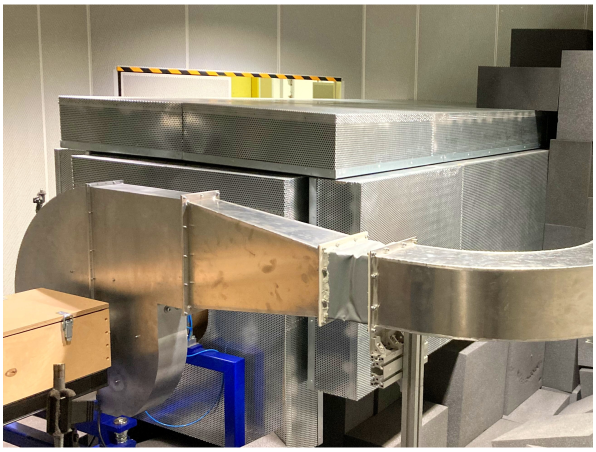

Figure 1. Photograph of the centrifugal test fan and duct system.

3. SIMULATION MODELS

The measured data should be reproduced by numerical simulations. For this purpose, FE models for the interior acoustic field and the mechanical field, as well as the exterior sound field, were set up. Two types of models are required. One high-fidelity model is backed by grid-refinement studies, and one low-fidelity model is used in the procedure of tuning the model parameters to satisfy the reference data. The solutions are computed for the time-harmonic case. The frequency band of interest is 20 Hz - 3000 Hz.

3.1 Method 1

Here, only the mechanical FE system should be calibrated, where the acoustic domain and the extended duct part are omitted. A unit normal force is applied to the same position as the hammer impact of the measurement. The time-harmonic structural vibration can be described by the Fourier-transformed linearized Navier's equation. Finite-element discretization and including a damping model leads to a system of equations of the form

$$\left(\underline{\boldsymbol{K}} - \mathrm{j}\omega\underline{\boldsymbol{C}} + \omega^2\underline{\boldsymbol{M}}\right)\underline{\boldsymbol{u}} = \underline{\boldsymbol{f}}, \tag{1}$$

where $\underline{\boldsymbol{K}}$, $\underline{\boldsymbol{C}}$, and $\underline{\boldsymbol{M}}$ are the stiffness, damping, and mass matrices, respectively. Furthermore, $\underline{\boldsymbol{u}}$ is the solution vector holding the mechanical displacements, $\underline{\boldsymbol{f}}$ the right-hand-side excitation vector, ω the angular frequency, and j the imaginary unit. The boundary conditions for Eqn. (1) are defined on the one hand by the natural (traction) boundary conditions arising due to the finite-element procedure. On the other hand, zero-displacement boundary conditions are set on all mounting positions of the construction and on the connecting surfaces to the omitted duct parts, respecting the direction of the opposing force.

In addition to the boundary conditions, the solution of Eqn. (1) depends on several material properties. Coefficients in the mass matrix are proportional to the material density ρ, while the stiffness-matrix coefficients are related to the elasticity modulus E_m and the Poisson ratio ν_P [4]. For the coefficients of the damping matrix, the most common approach is to exploit a linear combination of the stiffness and mass matrices (Rayleigh damping),

$$\underline{\boldsymbol{C}} = \alpha_R\underline{\boldsymbol{M}} + \beta_R\underline{\boldsymbol{K}}, \tag{2}$$

with the mass- and stiffness-proportional coefficients α_R and β_R, respectively. This leads to five parameters needed to be specified for an entirely unknown isotropic material: ρ, E_m, ν_P, α_R, and β_R.

The material properties are given to a sufficient extent in the datasheet of the main construction material, aluminum "AlMgSi1-3.2315". However, the exact material properties of the canvas sleeve and the plastic flanges of the sleeve connector are not known. Additionally, all flanges contain screws and are sealed by a thin rubber tape in between, features that are not included in the finite-element mesh. Also, the welding seams connecting the edges of the aluminum plates and the suspension behavior of the mountings might influence the solution.

The model validity at a single frequency can be indicated by considering the normalized root-mean-squared error (RMSE) of the transfer functions over all positions i on the measured surfaces,

$$\mathrm{RMSE}_\omega = \sqrt{\frac{\sum_i (H_{ref,i} - H_{sim,i})^2}{\sum_i H_{ref,i}^2}}, \tag{3}$$

where the transfer function is calculated from the surface-normal velocities divided by the normal excitation force,

$$H_i(\omega) = \frac{\boldsymbol{n}_i \cdot \boldsymbol{v}_i(\omega)}{f_{n,i}(\omega)}. \tag{4}$$

For calculating Eqn. (3) the transfer functions need to be determined on the same positions. Hence, the measured and simulated data needs to be interpolated to the cell centroids of the finite-element grid's outer surfaces and projected into the surface-normal direction beforehand. A k-nearest-neighbor interpolation with inverse-distance weighting was employed for this purpose, using the Python package pyCFS-data [5].

An initial simulation run of the high-fidelity model, where the canvas sleeve material was roughly estimated based on online available data sheets and the rest of the structure set to the properties of aluminum "AlMgSi1-3.2315" revealed an unsatisfactorily high RMSE over the investigated frequency range.

3.2 Method 2

The second validation method is complementary to method 1. Here, the mechanical FE model should produce sufficiently valid results already. The aim of method 2 is to include the left-out duct parts and the air domain to the calibration procedure. Here, the whole vibroacoustic FE model is solved, which leads to significantly higher computational cost. The loudspeaker is modeled as an acoustic normal-velocity boundary condition on the corresponding surface.

The direct-coupled vibroacoustic finite element simulation solves for Eqn. (1) and the system for the acoustic wave equation simultaneously. The system for the homogeneous acoustic wave equation in the time-harmonic case is of the form

$$\left(\underline{\boldsymbol{K}}_a + \omega^2 \underline{\boldsymbol{M}}_a\right) \boldsymbol{p} = \boldsymbol{0}, \tag{5}$$

where $\boldsymbol{p}$ holds the acoustic pressures. The systems are coupled by applying the correct interface conditions to the corresponding domain boundaries in the weak form [4]. Here, for a homogeneous fluid, the terms of the mass matrix are inversely proportional to the squared speed of sound, which can be specified via the mean fluid density ρ_0 and the compression modulus K, so that

$$c_0^2 = \frac{K}{\rho_0}. \tag{6}$$

Similarly to method 1, the model validity can be evaluated via the RMSE between measured and simulated results, Eqn. (3). Here, however, the excitation signal cannot be recorded from the loudspeaker. Hence, the frequency response of the loudspeaker mounted in a large baffle was determined in a separate laser-vibrometry measurement. As there is an expected deviation between the baffled and the duct-mounted frequency response, this topic is part of ongoing investigations.

4. OPTIMIZATION WORKFLOW

The model calibration should be done in three steps. First, evaluate the most relevant material parameters and boundary/interface conditions to vary in the mechanical model. Second, an optimized mechanical model can be determined via method 1. Third, calibration method 2 is used to optimize what is left: the acoustic material parameters and the extended duct.

For determining the most significant regions and material parameters to vary in the mechanical model, their effect should be tested with respect to the RMSE in method 1. For this purpose, the model is separated into multiple regions of different (effective) materials, which are sampled using Latin hypercube sampling and scaled to subjectively estimated bounds, considering available material catalogs and data sheets. For the boundary conditions modeling the suspension behavior of the mountings, spring elements can be applied and varied instead of using fixed boundary conditions.

Due to the initial high dimension of the parameter space and the high computation time required to solve for the mechanical FE model, the method for the significance ranking should be chosen carefully. The Spearman rank coefficient has been employed to evaluate correlations when the feature space is sparse. It is a non-parametric measure that assesses the strength and direction between two ranked variables [6]. Additionally, a Least Absolute Shrinkage and Selection Operator (LASSO) regression could be employed. This method is a form of regression that allows coefficients to shrink to zero. Thus, it is especially useful for variable selection and sparsely sampled data [7]. As a third method, the feature-importance values of a trained random forest (RF) regression model can be used to rank the feature significance. RF regressors are robust to overfitting and inherently handle non-linear relationships and interactions between variables [8]. Combining these three methods is expected to provide a robust significance estimation, even when applied to sparsely sampled data.

After reducing the feature space to sufficiently few features, optimization can be performed by using the trained RF regressor as a surrogate model and determining the optimized parameter set for a minimum RMSE. The optimization can be done, e.g., by exploiting a stochastic optimization algorithm.

5. CHALLENGES FOR THE METHOD

The major challenge of the optimization is the exceedingly high computational cost of evaluating the FE simulations. Hence, it is not feasible to evaluate the eigenfrequencies of the system via an eigenvalue analysis or to compute the full frequency band of interest in a sufficient resolution. Additionally, the low-fidelity model, which is required to save computation time, deviates significantly from the high-fidelity model for higher frequencies. Further, the measured transfer functions yield insufficiently high noise rates at frequencies below 60 Hz. For the calibration method 2, the unknown excitation of the loudspeaker might impact the result. Finally, the high initial RMSE of the mechanical simulation complicates the determination of significant variables and optimized solutions.

A first attempt to optimize the mechanical FE model was already conducted. Here, only seven frequencies in non-integer ratios ranging between 70 Hz and 780 Hz were simulated. Only material parameters, but no boundary conditions, varied. The procedure was conducted in three rounds of 650 simulation evaluations. The first two rounds were used to reduce the feature space from initially 65 to 13 features. The third round was then used to determine optimized parameters. This first attempt did not lead to satisfactory results.

6. CONCLUSIONS AND OUTLOOK

This proceeding discusses the workflow to calibrate the vibroacoustic system for a thin-walled duct system and the housing of a centrifugal fan. It documents the current state of a work in progress and outlines methods and difficulties for achieving the goal of a calibrated simulation model.

7. ACKNOWLEDGMENTS

This research was funded in whole, or in part, by the Austrian Science Fund (FWF) [I 5515-N] and by the German Research Foundation (DFG) [468338100]. The computational results presented have been achieved, in part, using the software openCFS.

8. REFERENCES

[1] C. Burgess and R. Thomspon, "Practical consideration of noise from fans," in *INTER-NOISE and NOISE-CON Congress and Conference Proceedings*, 2014.

[2] A. Cummings, "SOUND TRANSMISSION THROUGH DUCT WALLS," *Journal of Sound and Vibration*, vol. 239, pp. 731–765, Jan. 2001.

[3] T. Uffinger, F. Czwielong, A. Renz, P. Heidegger, S. Schoder, M. Kaltenbacher, and S. Becker, "Development of a test rig for the investigation of flow-induced mechanisms of sound generation at radial fans," *Applied Acoustics*, vol. 211, p. 109553, 2023.

[4] M. Kaltenbacher, *Numerical Simulation of Mechatronic Sensors and Actuators: Finite Elements for Computational Multiphysics*. Berlin, Heidelberg: Springer Berlin Heidelberg, 2015.

[5] "pyCFS." `https://pypi.org/project/pyCFS/`, 2025. Accessed: 2025-04-01.

[6] J. H. Zar, "Spearman rank correlation," *Encyclopedia of Biostatistics*, 2005.

[7] C. S. Signorino and A. Kirchner, "Using lasso to model interactions and nonlinearities in survey data," *Survey Practice*, vol. 11, pp. 1–10, 2018.

[8] G. Biau and E. Scornet, "A random forest guided tour," *Test*, vol. 25, pp. 197–227, 2016.